Nonlin. Processes Geophys., 17, 697–714, 2010
www.nonlin-processes-geophys.net/17/697/2010/
doi:10.5194/npg-17-697-2010

Nonlinear Processes in Geophysics

Multifractality, imperfect scaling and hydrological properties of rainfall time series simulated by continuous universal multifractal and discrete random cascade models

F. Serinaldi

Dipartimento di Geologia e Ingegneria Meccanica, Naturalistica e Idraulica per il Territorio – GEMINI, Università della Tuscia, Via S. Camillo de Lellis snc, 01100 Viterbo, Italy

Received: 8 April 2010 – Revised: 20 September 2010 – Accepted: 26 November 2010 – Published: 8 December 2010

Abstract. Discrete multiplicative random cascade (MRC) models were extensively studied and applied to disaggregate rainfall data, thanks to their formal simplicity and the small number of involved parameters. Focusing on temporal disaggregation, the rationale of these models is based on multiplying the value assumed by a physical attribute (e.g., rainfall intensity) at a given time scale L, by a suitable number b of random weights, to obtain b attribute values corresponding to statistically plausible observations at a smaller L/b time resolution. In the original formulation of the MRC models, the random weights were assumed to be independent and identically distributed. However, for several studies this hypothesis did not appear to be realistic for the observed rainfall series as the distribution of the weights was shown to depend on the space-time scale and rainfall intensity. Since these findings contrast with the scale invariance assumption behind the MRC models and impact on the applicability of these models, it is worth studying their nature. This study explores the possible presence of dependence of the parameters of two discrete MRC models on rainfall intensity and time scale, by analyzing point rainfall series with 5-min time resolution. Taking into account a discrete microcanonical (MC) model based on beta distribution and a discrete canonical beta-logstable (BLS), the analysis points out that the relations between the parameters and rainfall intensity across the time scales are detectable and can be modeled by a set of simple functions accounting for the parameter-rainfall intensity relationship, and another set describing the link between the parameters and the time scale. Therefore, MC and BLS models were modified to explicitly account for these relationships and compared with the continuous in scale universal multifractal (CUM) model, which is used as a physically based benchmark model. Monte Carlo simulations point out that the dependence of MC and BLS parameters on rainfall intensity and cascade scales can be recognized also in CUM series, meaning that these relations cannot be considered as a definitive sign of departure from multifractality. Even though the modified MC model is not properly a scaling model (parameters depend on rainfall intensity and scale), it reproduces the empirical traces of the moments and moment exponent function as effective as the CUM model. Moreover, the MC model is able to reproduce some rainfall properties of hydrological interest, such as the distribution of event rainfall amount, wet/dry spell length, and the autocorrelation function, better than its competitors owing to its strong, albeit unrealistic, conservative nature. Therefore, even though the CUM model represents the most parsimonious and the only physically/theoretically consistent model, results provided by MC model motivate, to some extent, the interest recognized in the literature for this type of discrete models.

Correspondence to: F. Serinaldi
(f.serinaldi@unitus.it)

1 Introduction

Rainfall series spanning several years are usually available at coarse time scales, say above daily resolution, thanks to the rain gauge networks operating over a long time. Similarly, rain fields at coarse space scale are provided by numerical weather prediction models and remote sensor instruments, such as radar and satellite. However, the space-time resolution of this data is often not appropriate for several hydrological analyses, and rainfall information needs to be disaggregated to a finer space-time resolution (e.g., Gaume et al., 2007). The problem has been widely studied in the literature

and several techniques have been proposed (see e.g., Koutsoyiannis et al., 2003; Sivakumar and Sharma, 2008; Rupp et al., 2009, and references therein). One of the most studied approaches is based on the discrete multiplicative cascades (e.g., Mandelbrot, 1974). The rationale of this method is to split each time (or space) interval at a given resolution and cascade level $k-1$ into a number b of subintervals at level k, and assign to each subinterval a rainfall value obtained by multiplying the rainfall intensity (or amount) of the parent coarse interval by the cascade weights W (also known as generator), which fulfill some prescribed properties recalled in the next sections. The process is repeated for a number of levels until the rainfall series/field is disaggregated to the required space/time resolution. In time series disaggregation, the branching number b is commonly assumed to be equal to 2, resulting in a dyadic cascade, so that the time scale is halved at each cascade level. In this case, after k levels, each interval at the reference (coarse) time scale L_0 is divided as $i = 1,2,...,b^k$ subintervals at finer scale L_k; therefore, the scale ratio is defined as $\lambda_k = L_0/L_k = b^k$ ($\lambda_0 = 1$ is associated with the 0th cascade level corresponding to the coarsest reference time scale L_0). The rainfall intensity R contained in the ith subinterval at a generic cascade level k is given by:

$$R_{i,k} = R_0 \prod_{j=1}^{k} W_j(i) = A_{i,k}\lambda_k \quad \text{for } i = 1,2,...,b^k;\ k > 0, \quad (1)$$

where $A_{i,k}$ is the rainfall amount corresponding to $R_{i,k}$, and the expectation of W is $E[W] = 1$. MRC models can be classified into two main groups, microcanonical and canonical, according to different conservation laws that characterize the cascade. In thermodynamics, the first type refers to an exact conservation of the energy at each cascade stage, and is appropriate for closed systems, while the latter preserves the ensemble averages, and is appropriate for open systems (e.g., Schertzer and Lovejoy, 1987). Since the atmospheric turbulence, rainfall, and other geophysical processes interact with each other and the external environment, the microcanonical constraint appears highly artificial and such models should be considered essentially academic. The most important consequence of the microcanonical constraint is that the model necessarily returns upper bounded singularities, limiting the occurrence of extreme realizations (e.g., Schertzer et al., 1991; Schertzer and Lovejoy, 1992; Lovejoy and Schertzer, 1995).

The interest in discrete MRC models is related to their simplicity compared to more complex approaches, as well as to their link to the energy transfer processes in turbulent flows (Kolmogorov, 1941, 1991; Schertzer and Lovejoy, 1987; Veneziano et al., 2006; Paulson and Baxter, 2007). However, these models can be considered as the "first generation" of MRC models (Lovejoy and Schertzer, 2010a), while more realistic results are provided by the "second generation" of continuous in scale multifractal processes based on Lévy stable random variables (e.g., Schertzer and Lovejoy, 1987, 1997; Lovejoy and Schertzer, 1995; Lovejoy et al., 2008). The latter models are called continuous universal multifractal (CUM) models owing to their properties of stability and attractivity, which correspond to a generalization of the central limit theorem (e.g., Schertzer and Lovejoy, 1987, 1997; Schertzer et al., 2010). Nevertheless, discrete MRC models are still widely applied and studied in the literature.

A basic hypothesis under the multiplicative structure in Eq. (1) is that the weights W are assumed to be independent and identically distributed (iid). However, as discussed by Veneziano et al. (2006), even though the multiplicative combination of the weights W is generally supported by empirical evidence (Menabde et al., 1997; Veneziano et al., 2006), commonly the iid assumption does not seem to be realistic. Cascade weights have been found to be dependent on scale (Veneziano et al., 1996; Menabde et al., 1997; Menabde and Sivapalan, 2000; Molnar and Burlando, 2005; Paulson and Baxter, 2007), on covariates such as large-scale rainfall intensity (Over and Gupta, 1994, 1996; Deidda, 2000; Molnar and Burlando, 2005), and on the interval class, i.e. intervals at the beginning, middle, or end of a rainfall event (Olsson, 1998; Olsson and Berndtsson, 1998; Güntner et al., 2001; Veneziano and Iacobellis, 2002).

Veneziano et al. (2006) have explored the dependence of the cascade weights on rainfall intensity and cascade level, assuming the so-called discrete canonical logstable model, which accounts for zero rainfall (hereinafter, also denoted as lacunarity) thanks to a thresholding procedure, and the beta-logstable (BLS) model (described in Sect. 2.2), which describes lacunarity by a parameter driving the rain/no-rain process. Since conditioning the weights to intensity results in biased estimates of the model parameters, Veneziano et al. (2006) suggested an iterative estimation procedure. Furthermore, they compared different versions of the BLS model, whose parameters may or may not vary with the rainfall intensity and/or the cascade level.

Rupp et al. (2009) have studied the relationships among weights, rainfall intensity, and cascade level by assuming a discrete two-parameter microcanonical model (see Sect. 2.3), with one parameter driving the lacunarity and the other controlling the generation of positive rainfall values. This model, with parameters depending on large-scale rainfall intensity, has been studied and applied by Over and Gupta (1994) to radar-derived rainfall maps, and by Molnar and Burlando (2005) to point rainfall series. Rupp et al. (2009) have found that the dependence between the lacunarity parameter and rainfall intensity can be properly described by a lognormal distribution, whose parameters vary in turn with the scale through power-law relationships, whereas the second parameter of the MC model can be described by quadratic functions of rainfall intensity, rescaled across the disaggregation levels. The idea behind the approach suggested by Rupp et al. (2009) is to describe the dependence between the MRC

model parameters and rainfall intensity by simple analytical functions, such as lognormal distribution or parabolic function, whose coefficients rescale in turn across the cascade levels, accounting for the scale dependence. Rupp et al. (2009) have noted that conditioning the weights to rainfall intensity may account for much of the dependence on interval class because the intensity is operatively discretized in classes for computational reasons. Hence, this approach encompasses in some way the classification strategy used by Olsson (1998), for example.

It should be noted that the studies by Veneziano et al. (2006) and Rupp et al. (2009) have different scopes. Veneziano et al. (2006) aimed at proving that the observed dependence of the cascade weights on rainfall intensity and cascade level cannot be reproduced by models that do not explicitly account for it, concluding that this behavior is not a spurious effect, but is related to the nature of the rainfall observations. In more detail, the observed precipitation can be considered as the flow of condensed water through a constant-altitude plane. Even though the rate of water vapor condensation is multifractal owing to its link to atmospheric turbulence, Veneziano et al. (2006) argued that the multifractality can be lost in the observation of condensed particles as rainfall measured at a constant altitude. On the other hand, Rupp et al. (2009) aimed at assessing the possible improvement in performance of the MC model, when the observed dependences of the cascade weights on rainfall intensity and cascade level are explicitly modeled, regardless of the nature of these relations.

The scope of the present study is to select and set up the most simple and possibly accurate MRC model that can simulate synthetic series useful as input for rainfall-runoff models. Thus, the focus is on the reproduction of several properties of hydrological interest, such as event rainfall amount and wet/dry spell length. Nevertheless, as the model selection is based on the analysis of the multifractal properties of observed rainfall series, the study also explores the dependence of the cascade weights on rainfall intensity and cascade level. The analysis relies on three rainfall series with a 5-min resolution from three rain gauges located in the Viterbo province (central Italy). Based on these data, the approach suggested by Rupp et al. (2009) was applied to both MC and BLS models to carry out comparisons and possible generalizations. For example, unlike Rupp et al. (2009), we found that the relationships between the parameters controlling the lacunarity and rainfall intensity could be modeled by a single power-law curve, resulting in more parsimonious models. Moreover, the CUM model is applied as a physically based multifractal benchmark model, and the corresponding multifractal exploratory analysis is used to study the nature of the observed dependence of the cascade weights on rainfall intensity and cascade level.

The article is organized as follows. In Sect. 2, the multifractal notation and the structure of the CUM, MC, and BLS models are briefly recalled. Section 3 describes multifractal analysis, and the empirical parameter-intensity-scale relationships are explored and parameterized. In Sect. 4, the performances of the considered models are assessed by comparing several statistics computed on the observed and simulated series. The conclusions are summarized in Sect. 5.

2 Basic multifractal concepts and MRC models

2.1 Multifractal formalism and continuous universal multifractal (CUM) model

In this study, the multifractal analysis focuses on rainfall intensity R, in agreement with the "codimension multifractal formalism" (Schertzer and Lovejoy, 1987), which is based on the statistics of densities of measures (here, the rainfall amount per time unit), and is well suited for analyzing stochastic multifractals. Informally, defining the scale invariance of R means to identify similarities in the statistical properties of the distribution function of R at different scales of aggregation. Once these common characteristics are found between two time scales, the variable R is said to be scale invariant, and statistical information about the distribution of R at the smallest resolution may be derived from coarse resolution characteristics (Mascaro et al., 2010).

In order to analyze the scaling properties of R, the data are aggregated to lower and lower resolution by temporal averaging. This "dressing" procedure is an attempt to invert the cascade "bare" process which we are interested in (e.g., Lovejoy et al., 2008). Denoting the reference external scale of the cascade by L_{ref} (here, $1280\,\text{min} \approx 1$ day), the generic aggregated scale by L (here, $L \in [5, 1280]$ min), and the scale ratio by λ, the scaling behavior entails:

$$\left\langle R_\lambda^q \right\rangle = \lambda^{K(q)} \langle R_1 \rangle^q; \quad \lambda = L_{\text{ref}}/L, \tag{2}$$

where $\langle \cdot \rangle$ denotes the ensemble mean, $\langle R_1 \rangle$ is the ensemble mean of R, the subscript "1" refers to the largest reference resolution corresponding to $\lambda = 1$, $K(q)$ is the moment scaling exponent, and q is the moment order. If $K(q)$ is constant, the process is said to be "simple scaling", otherwise R shows a "multiple scaling" behavior. It worth noting that L_{ref} is just a convenient scale, whereas, under scaling hypothesis, the cascade is characterized by an effective outer scale L_{eff} (the largest scale of variability) that is unknown a priori and should be estimated from the data (e.g., Lovejoy et al., 2008). Focusing on the normalized moments, from Eq. (2), it follows:

$$M_q = \frac{\left\langle R_\lambda^q \right\rangle}{\langle R_1 \rangle^q} = \lambda^{K(q)}. \tag{3}$$

The scaling of the moments can be assessed by computing M_q at different scales, and plotting M_q against the scale ratio λ in a log-log plane, where the power-law relation in Eq. (3) becomes linear. The empirical $K(q)$ functions can be estimated from the slopes of the trace moments (e.g., Schertzer and Lovejoy, 1987).

As mentioned in Sect. 1, in time series analysis, it is common to consider scales ratios multiple of $b = 2$. The choice of a discrete range of scales helps to understand cascade properties, is convenient for simulating, and is coherent with the dressing (averaging) procedure that is used to estimate M_q and $K(q)$. However, instead of considering a discrete cascade process evolving to its small-scale limit, it is possible to consider interactions of this process over a finite range of scales, with larger and larger numbers of its replicas, and then seek the small-scale limit (e.g., Schertzer and Lovejoy, 1987; Lovejoy and Schertzer, 1995; Schertzer and Lovejoy, 1997). This approach leads to CUM processes (Schertzer and Lovejoy, 1987). These processes are based on Lévy stable (or α-stable) random variables (e.g., Samorodnitsky and Taqqu, 1994) that follow the maximally asymmetric stable distributions with index of stability (or characteristic exponent) $\alpha \in (0,2]$ and skewness coefficient equal to -1 (e.g., Schertzer and Lovejoy, 1997). The corresponding theoretical $K(q)$ is a three-parameter function:

$$K(q) - qH = \begin{cases} \dfrac{C_1}{\alpha - 1}(q^\alpha - q), & \text{for } \alpha \neq 1 \\ C_1 q \log(q), & \text{for } \alpha = 1 \end{cases}, \tag{4}$$

where α is the above-mentioned index of stability, C_1 is the codimension of the mean singularity and describes the sparseness of the mean of process (e.g., Schertzer and Lovejoy, 1987; Tessier et al., 1993; de Lima and de Lima, 2009), and H is called the "nonconservation parameter", since $H \neq 0$ implies that the ensemble average statistics depend on the scale, while $H = 0$ is a quantitative statement of ensemble average conservation across the scales (e.g., Lovejoy and Schertzer, 1995; Lovejoy et al., 2008). It worth recalling that α values define five qualitative cases (Lovejoy and Schertzer, 1995): (1) $\alpha = 2$ defines multifractals with Gaussian generators; (2) $\alpha \in (1,2]$ defines multifractals with Lévy generators and unbounded singularities; (3) $\alpha = 1$ defines multifractals with Cauchy generators; (4) $\alpha \in (0,1)$ defines multifractals with Lévy generators and bounded singularities; (5) $\alpha = 0$ defines monofractal processes.

Unlike discrete cascades, the CUM theory implies simulation algorithms based on transformations in the frequency domain (fractional integrations) that allow the generation of rainfall sequences (or fields) at any (not necessarily integer) scale ratio λ. As the CUM model generates strictly positive realizations, the zero rainfall is introduced by assigning the zero value to the simulations below a minimum threshold. This is a simple but effective approach to account for deviations from a pure cascade behavior, based on the hypothesis that the scale breaks can be mainly ascribed to the minimum measurement resolution (e.g., Onof et al., 2005; Lovejoy et al., 2008). In this work, the simulation of causal CUM series (with corrections for finite size effects) was performed in R (R Development Core Team, 2009), by translating the Mathematica® codes provided by S. Lovejoy at the web site http://www.physics.mcgill.ca/~gang/multifrac/multifractals/software.htm. For further details on the implemented algorithms, the readers are referred to Wilson et al. (1991), and Lovejoy and Schertzer (2010a,b).

2.2 Discrete beta-logstable (BLS) canonical model

The development of a discrete multiplicative cascade in Eq. (1) requires the simulation of the weights W from a suitable distribution. Canonical and microcanonical models applied in this study differ in the distribution used to carry out the simulation. Canonical models are based on distributions with positive support and expected value $E[W] = 1$, which preserve the mass on an average at all levels in the cascade. In these models, the zero rainfall is accounted for by adopting discrete-continuous distributions $F(w) = p_0 + (1 - p_0)G(w)$, where $p_0 = \Pr[W = 0]$ and $G(w) = \Pr[W \leq w | W > 0]$. The probability p_0 describes the lacunarity and is related to the fractal dimension of the series, whereas the distribution G of the positive weights is often assumed to be lognormal (e.g., Gupta and Waymire, 1993; Molnar and Burlando, 2005), log-Poisson (e.g., Deidda et al., 1999, 2006; Deidda, 2000; Onof et al., 2005; Sivakumar and Sharma, 2008; Mascaro et al., 2010) or logstable (e.g., Schertzer and Lovejoy, 1987; Olsson, 1995; Pathirana et al., 2003; Veneziano et al., 2006). It should be noted that the hypothesis of existence of a fractal support is alternative to the assumption of a low threshold for the measurable rainfall intensity, allowing for a cross-check of the two hypotheses. Moreover, we recall that the terms "lognormal" and "logstable" are not strictly correct as the dressed process is only approximately logstable/lognormal for low-order moments or low singularities (Schertzer and Lovejoy, 1997). Nevertheless, since the discussion on the BLS model is based on the work by Veneziano et al. (2006), we adopt the definition "beta-logstable".

The theoretical $K(q)$ function corresponding to the BLS model is:

$$K(q) = \begin{cases} \beta_{\mathrm{BLS}}(q-1) + \dfrac{C_{\mathrm{BLS}}}{\alpha_{\mathrm{BLS}} - 1}(q^{\alpha_{\mathrm{BLS}}} - q), & \text{for } \alpha_{\mathrm{BLS}} \neq 1 \\ \beta_{\mathrm{BLS}}(q-1) + C_{\mathrm{BLS}} q \log(q), & \text{for } \alpha_{\mathrm{BLS}} = 1 \end{cases}, \tag{5}$$

where β_{BLS} is the parameter controlling zero rainfall. β_{BLS} is related to p_0 and fractal dimension D by the relationship $\beta_{\mathrm{BLS}} = -K(0) = -\log_b(1 - p_0) = d - D$, where d is the Euclidean embedding dimension of the rainfall process ($d = 1$ for a time series) (e.g., Over and Gupta, 1994, 1996; Veneziano et al., 2006). The second term in the right hand side of Eq. (5) has the same form as that of the right hand side of Eq. (4). However, in this study, the BLS parameters are assumed to vary with the discrete scale ratio λ_k (or cascade level k) and rainfall intensity of the parent intervals at

level $k-1$. Since the physical meaning of the index of stability and codimension is lost in this conditioning procedure, the parameters are denoted as C_{BLS} and α_{BLS} instead of C_1 and α. Moreover, the BLS model with scale-intensity varying parameters only preserves the dyadic structure of a discrete MRC model, but it is not actually a multifractal model at all. Indeed, its good performance (compared to a thresholded discrete logstable) is interpreted by Veneziano et al. (2006) as an indicator of departure from multifractality.

The estimation of BLS parameters requires the computation of the weights W, namely, the ratios between the rainfall intensity in a given subinterval at level k and the corresponding parent interval at level $k-1$. As the bare process $R_{\mathrm{b},k}$ is not really observed, weights W can only be estimated by the reverse dressed process R_k. In general, the statistics of the bare rainfall provide biased estimates of the dressed rainfall, and vice versa (e.g., Lovejoy and Schertzer, 1995; Veneziano et al., 2006; Paulson and Baxter, 2007). In order to correct this bias, Veneziano et al. (2006) have applied an iterative estimation procedure that adjusts the parameters estimated on the dressed process so that the $K(q)$ function of the simulated (disaggregated) series reproduces that of the observed series. Paulson and Baxter (2007) have used a similar approach, wherein, the objective function of an optimization process is the sum of the absolute differences between the second and third moments of the measured rainfall time series across the considered scales. In this study, to point out the impact of the model structure (canonical and microcanonical) on the bias of the estimates, any bias correction is applied.

To explore the possible dependence of BLS parameters on scale level and rainfall intensity, the empirical $K(q)$ function $K(q|k,R_{\mathrm{b},k-1})$ conditioned to scale level k and bare rainfall intensity $R_{\mathrm{b},k-1}$ is estimated as:

$$\hat{K}(q|k,R_{k-1}) = \log_b(\langle W^q(k,R_{k-1})\rangle) = \log_b\left(\frac{\langle R_k^q|R_{k-1}\rangle}{R_{k-1}^q}\right), \quad (6)$$

where $\langle R_k^q|R_{k-1}\rangle$ is the empirical qth moment of the conditional rainfall intensity $R_k|R_{k-1}$, and the range of R_{k-1} is partitioned in a suitable number of classes (Veneziano et al., 2006). For each scale level k and each R_{k-1} class, the $K(q)$ function of the BLS model in Eq. (5) is fitted to the empirical $\hat{K}(q|k,R_{k-1})$ (Eq. 6) by estimating the three parameters β_{BLS}, C_{BLS}, and α_{BLS}. β_{BLS} is assessed by the relationship $\beta_{\mathrm{BLS}} = -K(0)$, whereas, the other two parameters are estimated by the nonlinear least square minimization of the residuals $(K(q)-\hat{K}(q))$ (Dennis et al., 1981) computed over a range of moments $q \in [0,3]$. The procedure yields a set of three parameter estimates $\{\hat{\beta}_{\mathrm{BLS}}, \hat{C}_{\mathrm{BLS}}, \hat{\alpha}_{\mathrm{BLS}}\}$ for each combination of scale level k and class of rainfall intensity. For further details on the estimation method, the readers are referred to Sect. 3.2 and Veneziano et al. (2006).

2.3 Discrete microcanonical (MC) model

Unlike the canonical models, the microcanonical models preserve the exact mass of rainfall across the cascade levels. In this case, each parent interval at level $k-1$ is subdivided into b subintervals at level k, which contain a rainfall amount equal to the parent interval. In terms of rainfall intensity, this means that the generator W can be considered a random variable ranging in $[0,b]$ such that $\frac{1}{b}\sum_{i=1}^{b} W_k(i) = 1$ for each set of b subintervals at level k corresponding to a given parent interval at level $k-1$. For the sake of convenience, W is replaced with the rescaled $V = W/b$ ranging in $[0,1]$. Similar to the BLS model, the zero rainfall is explicitly preserved by allowing for $W = 0$ with a probability p_0. Assuming $b = 2$, as is done in this study, and denoting v_l and v_r as the weights of the left and right subintervals obtained from a parent interval, the probability that v_l and v_r are 0 or 1 is equal to the probability of the events $(v_l = 0 \wedge v_r = 1)$ or $(v_l = 1 \wedge v_r = 0)$ and is defined as $p_0 = \Pr[v_l = 0 \vee v_r = 0]$. Even though the probabilities of the events $(v_l = 0 \wedge v_r = 1)$ and $(v_l = 1 \wedge v_r = 0)$ are not necessarily equal, this property is empirically observed in several datasets (e.g., Molnar and Burlando, 2005; Rupp et al., 2009) and also in the data used in this study (figures not shown). Hence, the zero rainfall can be summarized by a unique parameter p_0 or $p_x = 1 - p_0$, where $p_x = \Pr[v_l \in (0,1) \wedge v_r \in (0,1)] = \Pr[v_l \in (0,1)] = \Pr[v_r \in (0,1)]$. The weights $V \in (0,1)$ are modeled by a symmetric one-parameter beta distribution:

$$f(v) = \frac{1}{B(a)} v^{a-1}(1-v)^{a-1}, \quad (7)$$

where $B(\cdot)$ is the beta function, and a is a shape parameter. This distribution is often used because it is defined on a finite support [0,1] and can assume several shapes, such as, uniform ($a = 1$), bell-shape ($a > 1$), and U-shape ($a < 1$). The distribution in Eq. (7) has mean $E[V] = 0.5$ so that $E[W] = 1$. For $b = 2$, pairs of weights v_l and v_r, which follow the distribution in Eq. (7) and fulfill the relation $v_l + v_r = 1$, can be simulated by drawing two independent realizations x_1 and x_2 from a gamma distribution with parameter a, and by taking the ratios $x_1/(x_1+x_2)$ and $x_2/(x_1+x_2)$ (Mood et al., 1974; Koutsoyiannis and Xanthopoulos, 1990). Parameter a can be estimated by the method of moments through the relationship $a = 1/(8\mathrm{Var}[V]) - 0.5$ (e.g., Molnar and Burlando, 2005). Analogous to BLS model, the parameter estimates are conditioned to the scale level k, and rainfall intensity R_{k-1} as follows: for a generic cascade level k, the range of rainfall intensities R_{k-1} at the previous stage $k-1$ (coarser resolution) is partitioned in a finite number of intensity classes; the intervals with R_{k-1} falling in a given class are taken, and the corresponding (disaggregated) subintervals at level k are used to estimate $p_x|R_{k-1}$ and $a|R_{k-1}$. The procedure yields a set of two parameters $\{\hat{p}_x, \hat{a}\}$ for each combination of scale level and intensity class. Following the approach of Rupp et al. (2009), the relationships between the MC parameters

Table 1. Annual summary statistics of the three stations Castel Cellesi (CCE), Montefiascone (MFI), and Viterbo (VIT).

Station	CCE	MFI	VIT
Elevation	369	560	357
Latitude	42.591	42.536	42.420
Longitude	−11.848	−11.973	−11.894
Mean [mm]	824	878	841
StDev [mm]	200	246	154
5th percentile [mm]	548	556	628
25th percentile [mm]	697	743	729
75th percentile [mm]	963	1072	932
95th percentile [mm]	1129	1267	1060

(p_x and a), scale level k, and rainfall intensity R_{k-1} are analyzed and modeled by analytical formulas.

3 Data analysis

The data analyzed in this study are from three 5-min rainfall series recorded in three stations (Castel Cellesi (CCE), Montefiascone (MFI), and Viterbo (VIT)) located in the Viterbo province (central Italy), by tipping bucket rain gauges with 0.2 mm resolution. The VIT time series spans from 1995 to 2005 (11 years), while CCE is available for 10 years (1995 to 2000, 2002, 2003, 2005, 2006) and MFI for eight years (1995 to 1997, 1999, 2002 to 2005). The corresponding daily series were studied and modeled by Serinaldi (2009), and the annual summary statistics are shown in Table 1. The lack of long continuous rainfall data at a fine time scale motivates the research on rainfall modeling and disaggregation to obtain the information required in hydrological studies. As disaggregation methods are often applied to downscale daily rainfall series, scales ranging from 5 min to 1280 min are used here because the latter is the scale closest to the 1440-min daily scale, achievable by aggregating 5-min series with $b = 2$ (e.g., Molnar and Burlando, 2005). For CUM simulation, this limitation does not apply; however, the same range of scales is used for the sake of comparison. Moreover, only results referring to the MFI data are presented in the following discussion, as similar conclusions hold for CCE and VIT series.

3.1 Multifractal analysis

The first analysis performed on the data aims at exploring the presence of an overall scaling behavior across a wide range of scales and the range of rainfall intensities. Therefore, the first multifractal analysis, which is related to CUM framework, is performed without splitting estimates as a function of scale and coarse rainfall intensity, whereas the possible dependence of the scaling properties on k and R_{k-1} is discussed in Sect. 3.2.

Figure 1a shows the power spectrum density (PSD) of the MFI time series at a 5-min resolution. The scaling behavior should result in a linear pattern of the PSD in log-log scale. The figure points out that the PSD is not strictly linear. However, taking into account that the PDS of rainfall series can be affected by a number of factors (e.g., Harris et al., 1997), the approximation is deemed reasonable for resolutions between 10 min and 1 day. The slope coefficient β of the straight line fitted to PSD is equal to 0.88, corresponding to a value of the Hurst exponent equal to 0.94. To check the sensitivity of this estimate, β was also estimated considering the PSD between 1 h and 1 month, obtaining a value equal to 0.68, and Hurst exponent equal to 0.84. Figure 1b shows the normalized moments of order q increasing from 0 to 3 by steps of 0.2. Even though the coarse reference scale is 1280-min, data have been aggregated up to ≈ 15 days to better appreciate the scaling behavior. The patterns are rather linear except for some unavoidable departures. Moments of low order do not converge to a fixed outer scale; however, as the order increases, the lines tend to converge to the scale ratio $\log_2(\lambda_{\text{eff}}) = \log_2(L_{\text{ref}}/L_{\text{eff}}) = \log_2(0.9/90) \approx -6.6$, meaning that $L_{\text{eff}} \approx 90$ days (3 months). The empirical $K(q)$ estimated from the slopes of the trace moments is shown in Fig. 1c. Zero rainfall and rounding off introduced by the resolution of the rain gauge result in an almost linear pattern of $K(q)$. The value $K(0)$ allows defining the codimension of the intervals with positive rainfall as $-K(0) \approx 0.47$ and the fractal dimension $D = 1 - 0.47 = 0.53$. The slope $K'(1)$ provides the codimension of the mean $C_1 \approx 0.38$. It should be noted that these values are coherent with those reported by Lovejoy and Schertzer (1995) for rain gauge daily rainfall data, de Lima and Grasman (1999) for 15-min and daily rainfall, and de Lima and de Lima (2009) for 10-min and daily rainfall. Assuming $C_1 \approx 0.38$ and $L_{\text{eff}} \approx 90$ days (=129 600 min), the equation $R_\lambda = \lambda^{C_1}\langle R_1\rangle$ gives that the main contribution to the mean R is $(129600/5)^{0.38} \approx 48$ times the mean, namely, $0.108 \cdot 48 \approx 5.2\,\text{mm h}^{-1}$.

Figure 1c also shows $K(q)$ corresponding to the process δR obtained by taking the absolute differences of R at the finest resolution. As the difference of the slopes $K'(q)$ of K_R and $K_{\delta R}$ is equal to H (e.g., Lovejoy et al., 2008), it can be used to check the value of H. For the data on hand, H ranges between -0.0036 and 0.0026, i.e. H can be assumed equal to zero. To compute the parameter α and to check the value of C_1, we have applied the double trace moment (DTM) method (e.g., Lavallée et al., 1991; Schmitt et al., 1992, 1993). Referring the readers to the mentioned references for technical details, the slopes of the straight lines in Fig. 1d give an estimate of α. As the intercepts correspond to the values of $K(q)$, estimates of C_1 can be obtained from Eq. (4) as $C_1 = K(q)(\alpha - 1)/(q^\alpha - q)$ for $H = 0$. For $q = \{1.5, 1.75, 2\}$, we obtain $\hat{\alpha} = \{0.812, 0.820, 0.804\}$ and $\hat{C}_1 = \{0.374, 0.371, 0.376\}$. The estimates of C_1 are coherent with the value obtained from the slope $K'(1)$, whereas $\hat{\alpha}$ values are only "guess" estimates, which were checked by

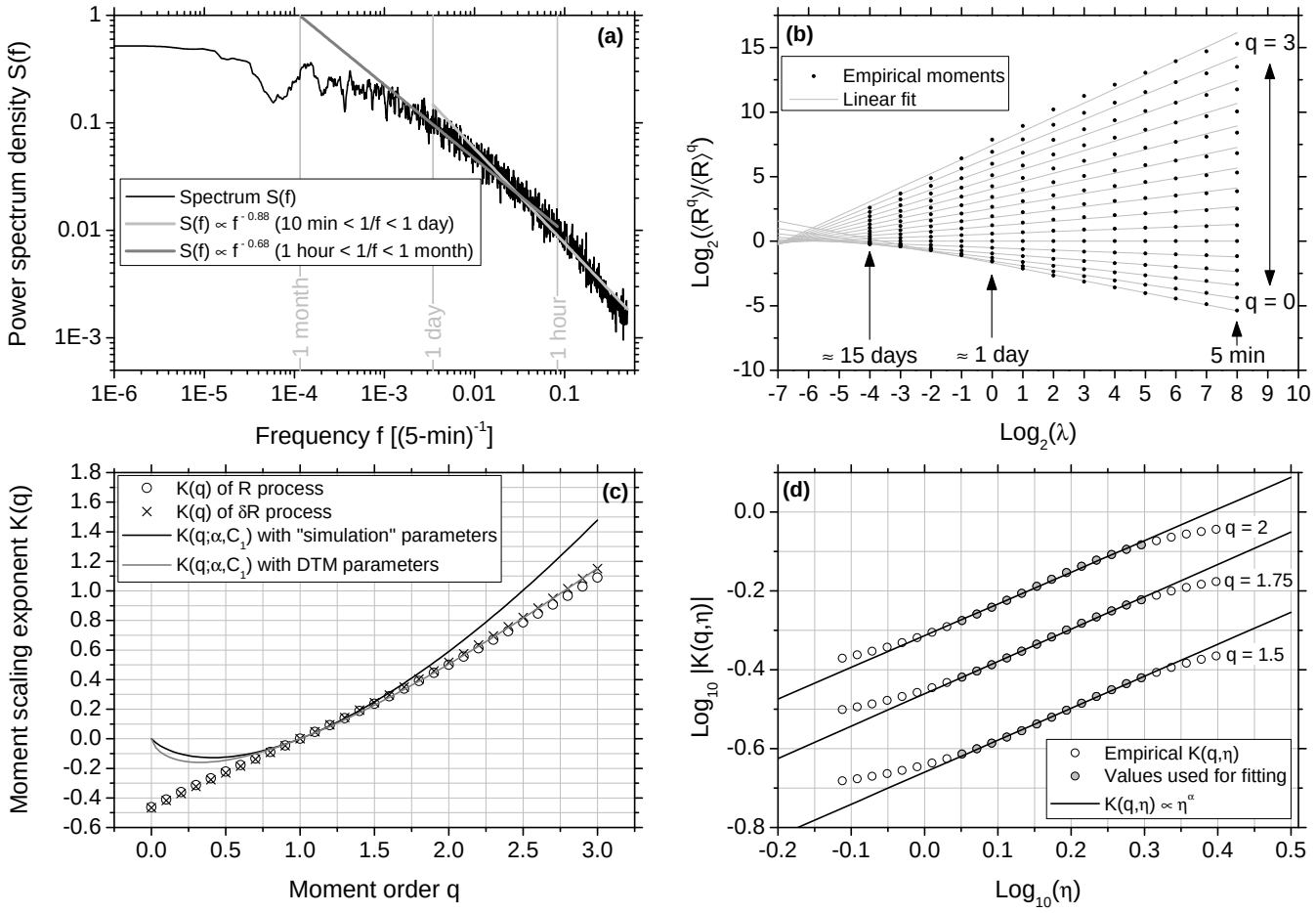

Fig. 1. **(a)** Power spectrum density (PSD) of the observed MFI series. Grey lines denote the power-law curves fitted on PSD for two different ranges of frequencies. **(b)** Traces of normalized moments, and corresponding moment-scale power-law relationships fitted to the data. **(c)** Empirical and CUM theoretical $K(q)$ functions. **(d)** Patterns of $|K(q,\eta)|$ resulting from the double trace moment (DTM) technique for $q = \{1.5, 1.75, 2\}$. Straight lines represent the power-law fitted to the linear part of the patterns (grey points).

simulation. The procedure leads to a final value, $\hat{\alpha} = 1.25$, which yields simulations with moment scaling behavior and $K(q)$ close to the observed series. It should be noted that the α values provided by DTM imply bounded singularities, while the final value obtained by simulation yields unbounded singularities. The theoretical CUM $K(q)$ functions with $C_1 = 0.38$ and α equal to 0.81 and 1.25 are shown in Fig. 1c: $K(q)$ with the parameter $\alpha = 0.81$ is very close to the empirical $\hat{K}(q)$, whereas the differences are more evident for the value $\alpha = 1.25$. In spite of this disagreement, in Sect. 4.1, it is shown that the value $\alpha = 1.25$ provides thresholded series that exhibit empirical $\hat{K}(q)$ close to the observed one.

Finally, an alternative estimate of H was performed by the relationship (e.g., Lovejoy and Schertzer, 1995):

$$H = \frac{\beta - 1 + K(2)}{2} = \frac{\beta - 1}{2} + \frac{C_1(2^{\alpha} - 2)}{2(\alpha - 1)}. \quad (8)$$

Assuming $\beta = 0.88$, Eq. (8) gives H values equal to ≈ 0.19 and ≈ 0.23 for $\alpha = 0.81$ and $\alpha = 1.25$, respectively. For $\beta = 0.68$ and the same values of α, $H \approx 0.09$ and ≈ 0.14. These values are within the ranges reported in the literature dealing with rainfall analysis (e.g., Royer et al., 2008; de Lima and de Lima, 2009), and are compatible with $H = 0$ owing to the low accuracy resulting from measurement discretization and seasonality (e.g., Lovejoy et al., 2008).

3.2 Analysis of imperfect scaling

As mentioned in Sect. 1, several studies have pointed out the dependence of discrete cascade parameters on scale level k and rainfall intensity R_{k-1}. To check the presence of these relations, the parameters of BLS and MC models were estimated by the method described in Sect. 2.2 and 2.3. In more detail, nine time scales from 1280 min (λ_0) to 5 min (λ_8) were considered. At each cascade level k, the weights W were computed from R_{k-1} and R_k, and the corresponding

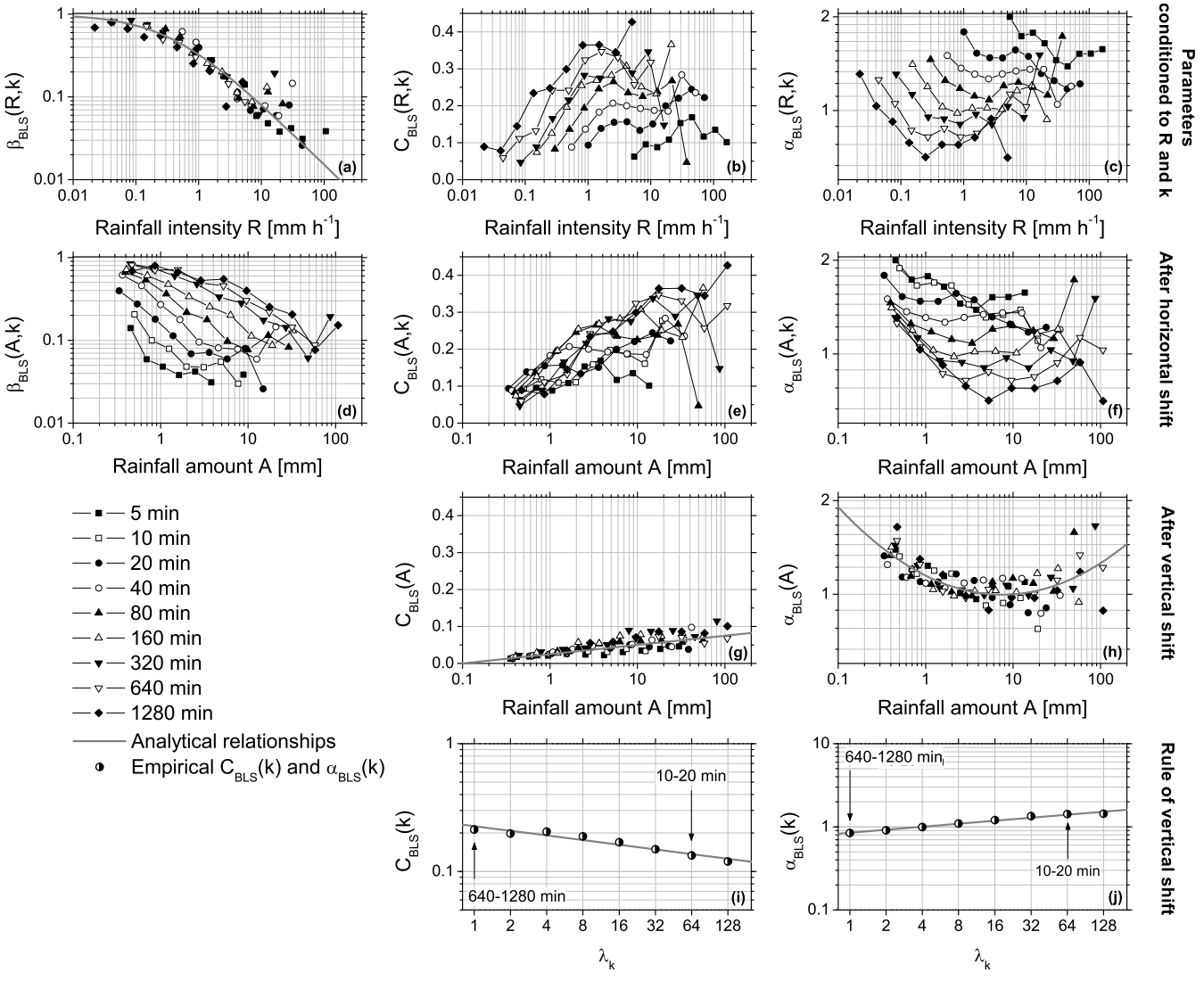

Fig. 2. Relationships among BLS parameters, time scale, and rainfall intensity R or amount A.

statistics were used to estimate BLS and MC parameters at level k. To study the possible dependence on the rainfall intensity of parent intervals, the range of R_{k-1} was partitioned in 12 classes (logarithmically binned). Therefore, for each level k, there are 12 subsets of R_{k-1} and the corresponding R_k, leading to 12 sets of parameters. This procedure allows studying the relation between the models' parameters and R_{k-1} at each scale level. Figure 2a–c shows the relationships between the BLS parameters and the rainfall intensity. The values of β_{BLS} are aligned along a rather well-defined pattern (Fig. 2a), which can be suitably parameterized by a power-law type function ranging in [0,1]:

$$\beta_{\mathrm{BLS}}(R) = \frac{1}{1+\sigma(R-\mu)^{\xi}}, \tag{9}$$

where μ, σ, and ξ are position, scale, and shape parameters, respectively. However, from Fig. 2a, the dependence on scale level is not clear. This dependence may be highlighted by performing a horizontal shift of the points in Fig. 2a proportional to the scale level, i.e. by transforming the rainfall intensity into rainfall amount $A_k = R_k/\lambda_k$. Figure 2d shows the result of the shifting procedure. The plot points out that β_{BLS} follows well-defined patterns for each cascade level, exhibiting a systematic decrease as the time scale decreases and rainfall amount increases. It is worth noting that each curve in Fig. 2d should show 12 points for each cascade level, according to the estimation procedure. However, at some scales, a smaller number of points are shown, since some R classes contain few values, resulting in unreliable estimates. As $R \geq 0$, it is assumed that $\mu = 0$. It follows that the dependence among β_{BLS}, rainfall intensity R, and scale level k can be summarized by a simple two-parameter power-law function of R.

The patterns of C_{BLS} (Fig. 2b) seem to increase as the time scale and rainfall intensity increase. However, a decreasing behavior emerges at the highest rainfall values. To parameterize these patterns, a double translation was performed. First, curves were horizontally translated by transforming the rain intensity into rainfall amount $A_k = R_k/\lambda_k$. Thus, we focus on the dependence of C_{BLS} on A instead of R (Fig. 2e). Therefore, the curves in Fig. 2e are collapsed by a vertical shift (Fig. 2g). This shift is preformed multiplying the values of each curve by the overall value of $C_{\mathrm{BLS}}(k)$, which is computed using all data R_{k-1} and R_k without partitioning the range of R_{k-1}. Points in Fig. 2g are approximately aligned along a straight line in the log-linear plane, which is modeled by a log-linear relationship:

$$C_{\mathrm{BLS}}(A) = c_0 + c_1 \log(A), \tag{10}$$

in which c_0 and c_1 denote generic coefficients. Figure 2i shows the values of the overall $C_{\mathrm{BLS}}(k)$ that are used to perform the vertical shift. $C_{\mathrm{BLS}}(k)$ is parameterized by a power-law function of λ_k:

$$C_{\mathrm{BLS}}(k) = d_0(\lambda_k)^{d_1}, \tag{11}$$

where d_0 and d_1 are coefficients to be estimated on the data. Since Eqs. (10) and (11) summarize the dependence of C_{BLS} on A and k, respectively, $C_{\mathrm{BLS}}(A,k)$ can be written as:

$$C_{\mathrm{BLS}}(A,k) = C_{\mathrm{BLS}}(A)/C_{\mathrm{BLS}}(k). \tag{12}$$

In other words, the curves in Fig. 2e can be modeled by an equation depending on A, which is properly shifted to account for the scale, according to the rule $C_{\mathrm{BLS}}(k)$.

A similar approach was applied to parameter α_{BLS}. Figure 2c points out that a horizontal shift coupled with a vertical shift can be appropriate to collapse the curves, allowing for the parsimonious modeling of α_{BLS}. Analogous to C_{BLS}, the horizontal shift is performed by transforming R_k in $A_k = R_k/\lambda_k$ (Fig. 2f). Therefore, the resulting curves are considered as realizations of a unique function $\alpha_{\mathrm{BLS}}(A)$ depending on A (Fig. 2h), which is shifted according to a coefficient $\alpha_{\mathrm{BLS}}(k)$ depending on k (Fig. 2j). $\alpha_{\mathrm{BLS}}(k)$ are the α_{BLS} parameters computed on the whole series at each cascade stage k, without partitioning R in 12 classes. $\alpha_{\mathrm{BLS}}(A)$ is described by a two-order polynomial (Fig. 2h):

$$\log(\alpha_{\mathrm{BLS}}(A)) = c_0' + c_1' \log(A) + c_2' (\log(A))^2, \tag{13}$$

in which c_0', c_1', and c_2' are the polynomial coefficients, and $\alpha_{\mathrm{BLS}}(k)$ is modeled by a power-law function of λ_k:

$$\alpha_{\mathrm{BLS}}(k) = d_0'(\lambda_k)^{d_1'}, \tag{14}$$

where d_0' and d_1' are the power-law coefficients. The parametric counterpart of the curves in Fig. 2f can be obtained by combining $\alpha_{\mathrm{BLS}}(A)$ and $\alpha_{\mathrm{BLS}}(k)$ according to the following multiplicative rule:

$$\alpha_{\mathrm{BLS}}(A,k) = \alpha_{\mathrm{BLS}}(A)\alpha_{\mathrm{BLS}}(k). \tag{15}$$

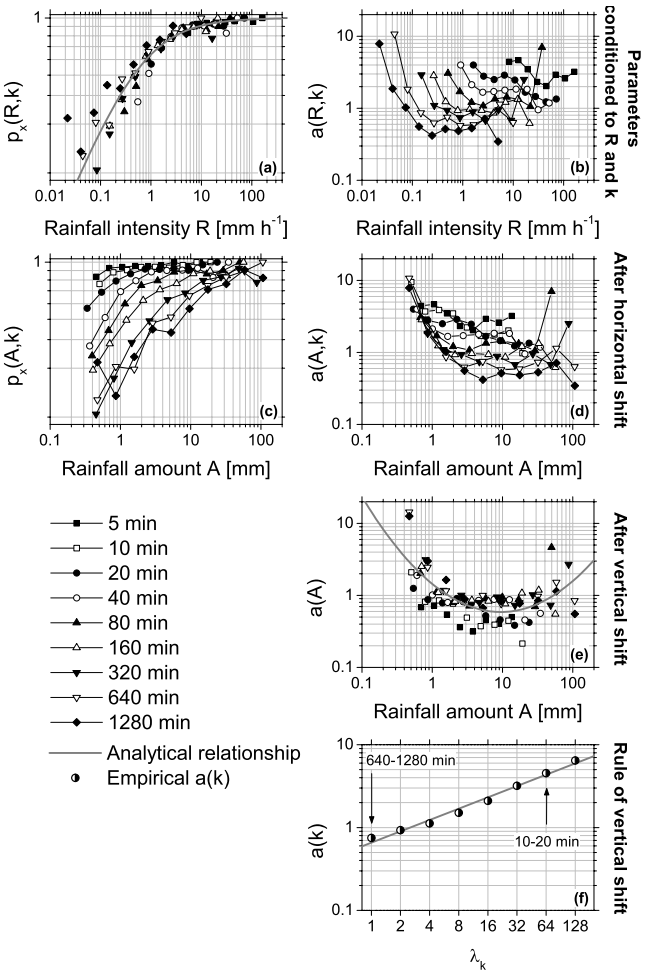

Fig. 3. Relationships among MC parameters, time scale, and rainfall intensity R or amount A.

The same method was applied to the MC parameters. In order to perform a comparison with the results obtained by Rupp et al. (2009), we focused on p_x instead of p_0. Unlike Rupp et al. (2009), who parameterized p_x by the lognormal distribution, whose coefficients varied with time scale through loglinear functions, we adopted a simpler approach. Figures 3a and 3c show that the patterns of $p_x(A,k)$ could be collapsed into a unique curve $p_x(R)$ by the same horizontal shifting procedure used for β_{BLS}. Hence, a power-law function was used:

$$p_x(R) = \frac{1}{1+\sigma'(R-\mu')^{\xi'}}. \tag{16}$$

where μ', σ', and ξ' are position, scale, and shape parameters, respectively. Analogous to α_{BLS}, the patterns of a (Fig. 3b) were shifted horizontally (Fig. 3d), and then vertically (Fig. 3e). The resulting (collapsed) patterns in Fig. 3e were described by a two-order polynomial:

$$\log(a(A)) = c_0'' + c_1'' \log(A) + c_2'' (\log(A))^2, \tag{17}$$

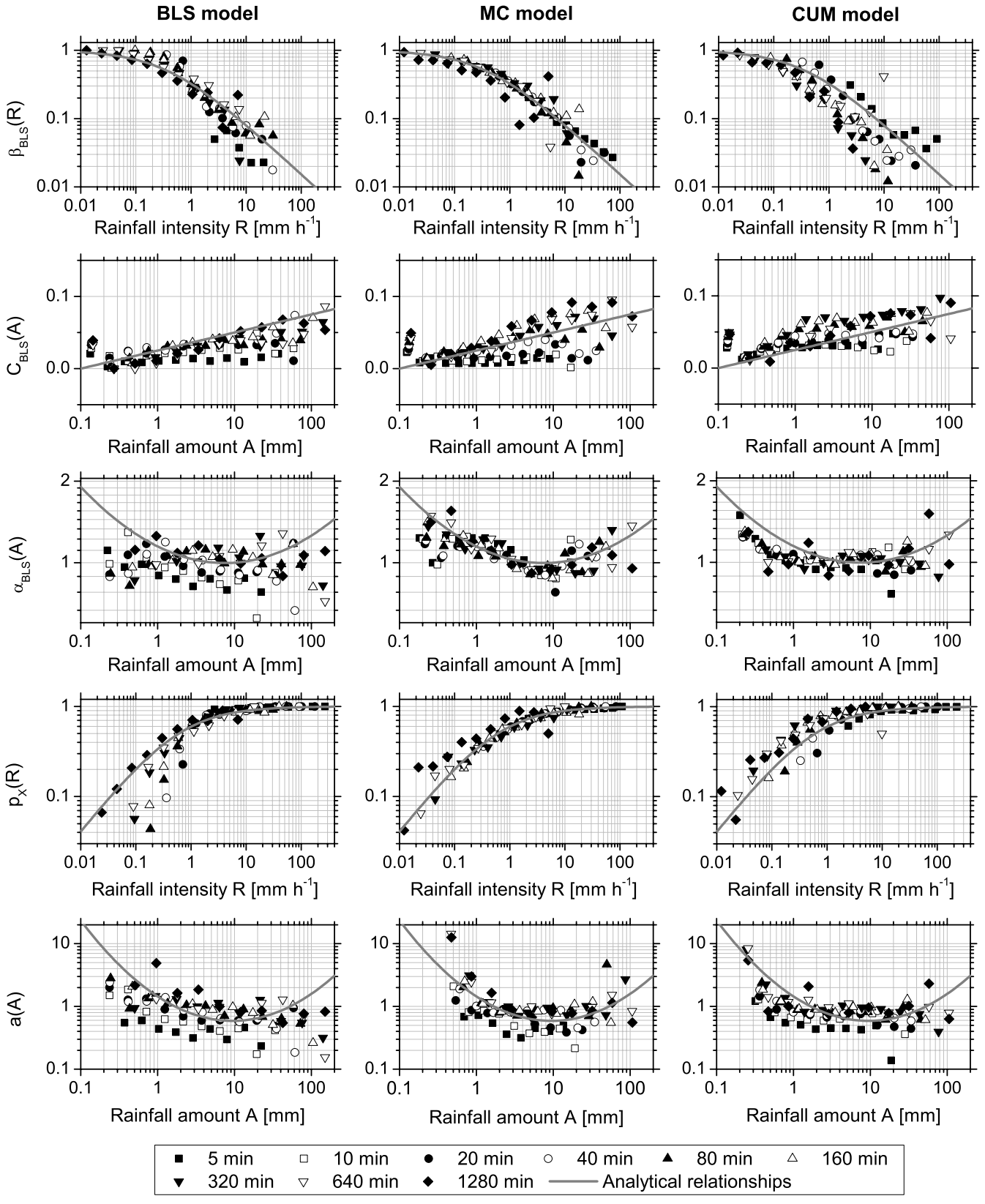

Fig. 4. Relationships between models' parameters and rainfall intensity (or amount) for three representative series simulated by BLS, MC, and CUM models.

while the rule that drives the vertical shift $a(k)$ was described by a power-law function of λ_k (see Fig. 3f):

$$a(k) = d_0''(\lambda_k)^{d_1''}. \quad (18)$$

The parametric counterpart of the curves in Fig. 3d can be obtained by combining $a(A)$ and $a(k)$ according to the following multiplicative rule (Rupp et al., 2009):

$$a(A,k) = a(A)a(k). \quad (19)$$

4 Simulations and results

The physically based CUM model and discrete BLS and MC models with parameters that vary according to Eqs. (9)–(19) have been applied to simulate 100 synthetic rainfall sequences at 5-min time scale with the same length of the observed series. In the CUM simulation, series were thresholded using a value equal to twice the observed mean ($2 \cdot 0.108\,\mathrm{mm\,h^{-1}}$). As in the previous section, only results referring to MFI series are reported. The performance of the models was assessed by comparing the ability to reproduce both the modeled parameters and scaling properties along with a number of rainfall characteristics useful for hydrological applications. Moreover, the possible presence of chaotic behavior was explored in order to evaluate the models in terms of properties not explicitly accounted for by CUM, BLS and MC model structures.

4.1 Scaling properties

First, we have evaluated the ability of the models to reproduce the analytical relationships (Eqs. 9–19) that describe the possible imperfect scaling. Figure 4 compares the relationship between the models' parameters and rainfall intensity R or rainfall amount A after removing the dependence on the scale level, i.e. after the vertical shift described in Sect. 3.2. The lines refer to analytical relationships with coefficients estimated on the MFI observed series, while empirical relationships associated with a representative simulated series are denoted with points. BLS and MC parameters were computed on CUM, BLS, and MC series, in order to assess if each model could reproduce the parameter patterns of the others. β_{BLS}, α_{BLS}, p_x, and a, corresponding to BLS series, appear to be more dispersed than those of MC series, whereas the BLS C_{BLS} values show some bias compared to the MC values. The most important result is that the CUM model is able to reproduce the parameter patterns quite well, except for some unavoidable bias. The relationship between scales and parameters driving the vertical shifts described in Sect. 3.2 is shown in Fig. 5. Also in this case, the bias of the parameters computed on the BLS series appears slightly more evident than that of the MC series. Even though the structure of the two-parameter CUM model does not explicitly account for the analytical patterns illustrated in the figure, it shows an agreement comparable to that of the more

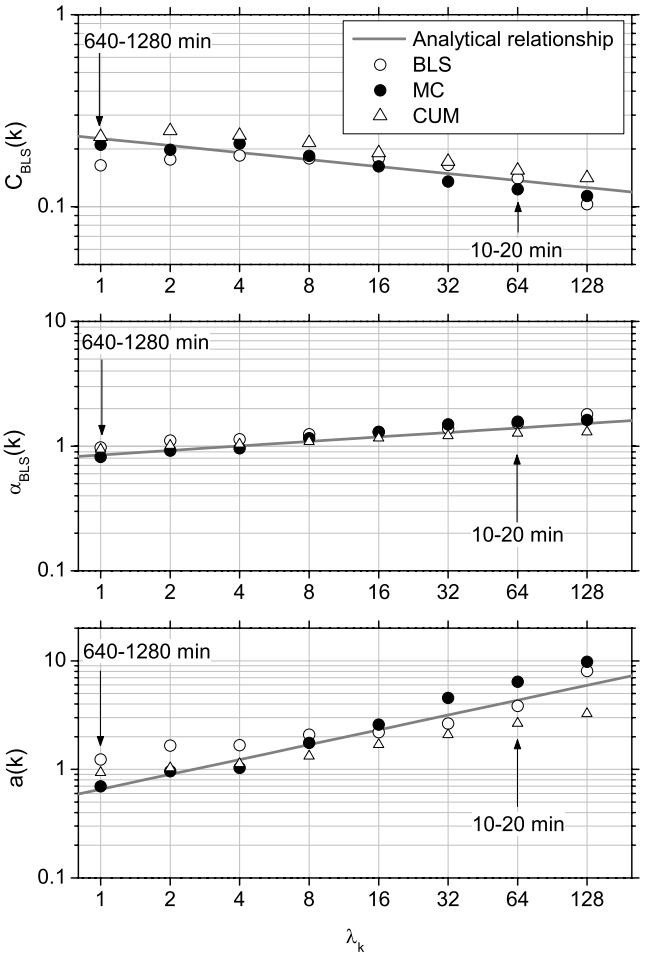

Fig. 5. Relationships between the models' parameters and scale for the representative series used in Fig. 4.

complex BLS and MC models. The systematic patterns in the models' parameters, which were detected in the time series, should be a sign of the changes in the distribution of W related to the cascade level and classes of rainfall intensity (or amount). However, as these patterns can be reproduced by a thresholded multifractal model (CUM), they cannot be considered as a definitive proof of the presence of physically based departures from multifractality.

MC, BLS, and CUM simulated series were also analyzed by the same multifractal techniques applied in Sect. 3.1. Figure 6 (top panels) shows the PSD of a representative simulated series for each model. BLS tends to overestimate the PSD, whereas MC shows the best agreement. This result is expected, and can be ascribed to the strong conservation rule that characterizes the MC model. A better performance of BLS could be obtained using the trial-and-error fitting procedure applied by Veneziano et al. (2006). However, as mentioned in Sect. 2.2, this approach was not used in order that the comparison between BLS and MC is not influenced by different estimation methods. CUM series exhibits a PSD

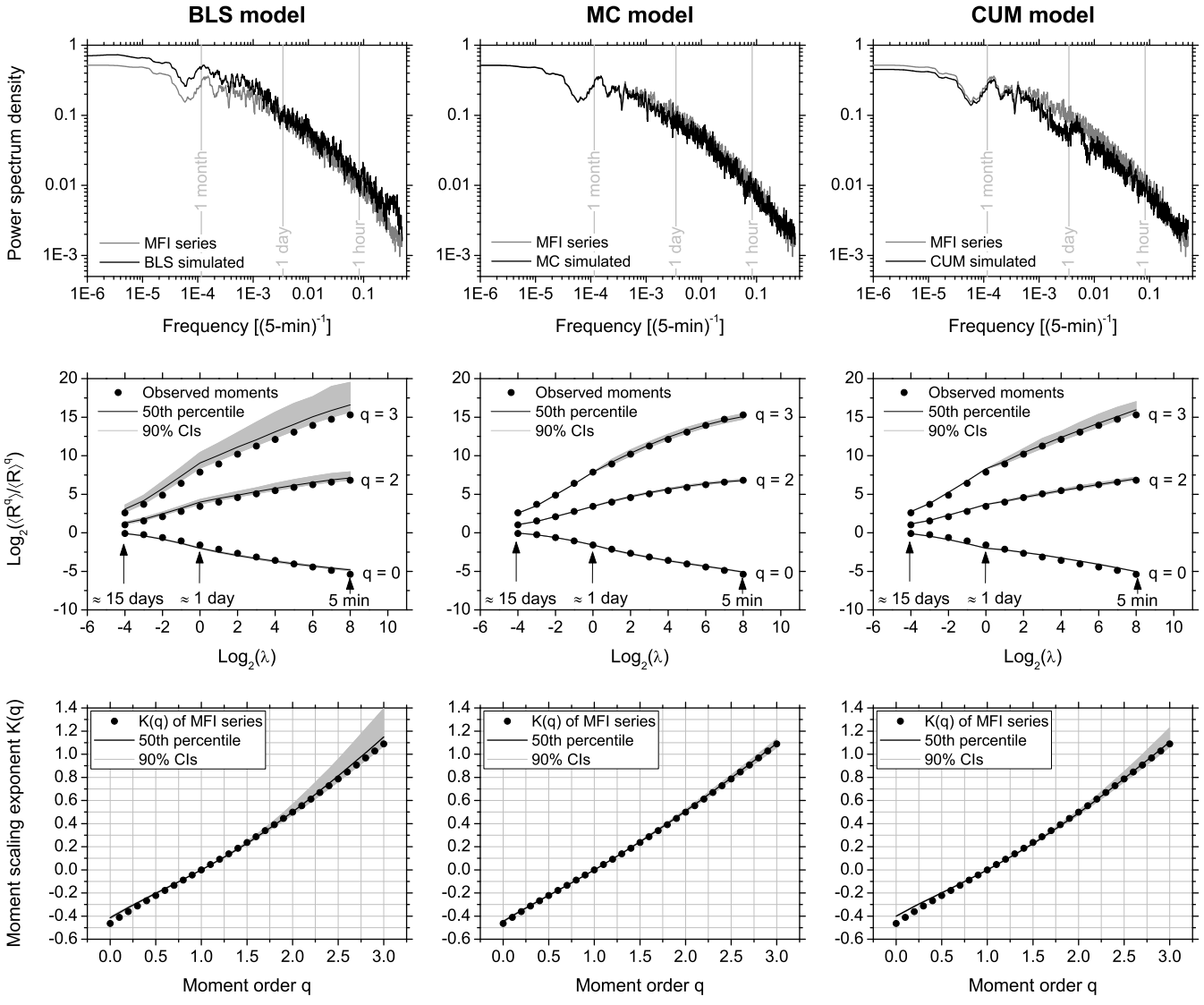

Fig. 6. Top panels show the PSD of three representative rainfall series simulated by BLS, MC, and CUM models (black lines) along with the PSD of the observed MFI series (grey lines). Middle panels show the traces of normalized moments of the observed MFI series (points) and the median patterns corresponding to the sequences simulated by the three models (lines). Grey areas denote the 90% confidence intervals (CIs) computed on 100 simulations. Bottom panels illustrate the $K(q)$ functions corresponding to the trace moments shown in the middle panels.

similar to the observed one but less accurate than the PSD of the MC series. Figure 6 also shows the traces of the moments of order $q = \{0, 2, 3\}$ (middle panels), and $K(q)$ functions (bottom panels). The graphs illustrate the median patterns and the 90% confidence intervals (CIs) computed from the 100 simulations. All models are able to reproduce low-order moments (say, $q < 2$), whereas differences are more evident for higher moments ($q > 2$). BLS exhibits both systematic bias and variance higher than MC and CUM. As expected, MC model yields series with statistical properties very close to the observed series owing to its strong conservative structure. On the other hand, the performance of CUM model is remarkable, considering its parsimonious structure based on two invariant parameters. The simple thresholding procedure mimics the fractal support of the observed series quite well. Unlike MC, CUM model (with $\alpha = 1.25$) involves unbounded singularities, resulting in a higher variability of the high-order moments.

4.2 Physical properties

As the main purpose of disaggregation is to obtain rainfall series at a fine time scale, to be used for further analyses, the BLS, MC and CUM models should provide synthetic

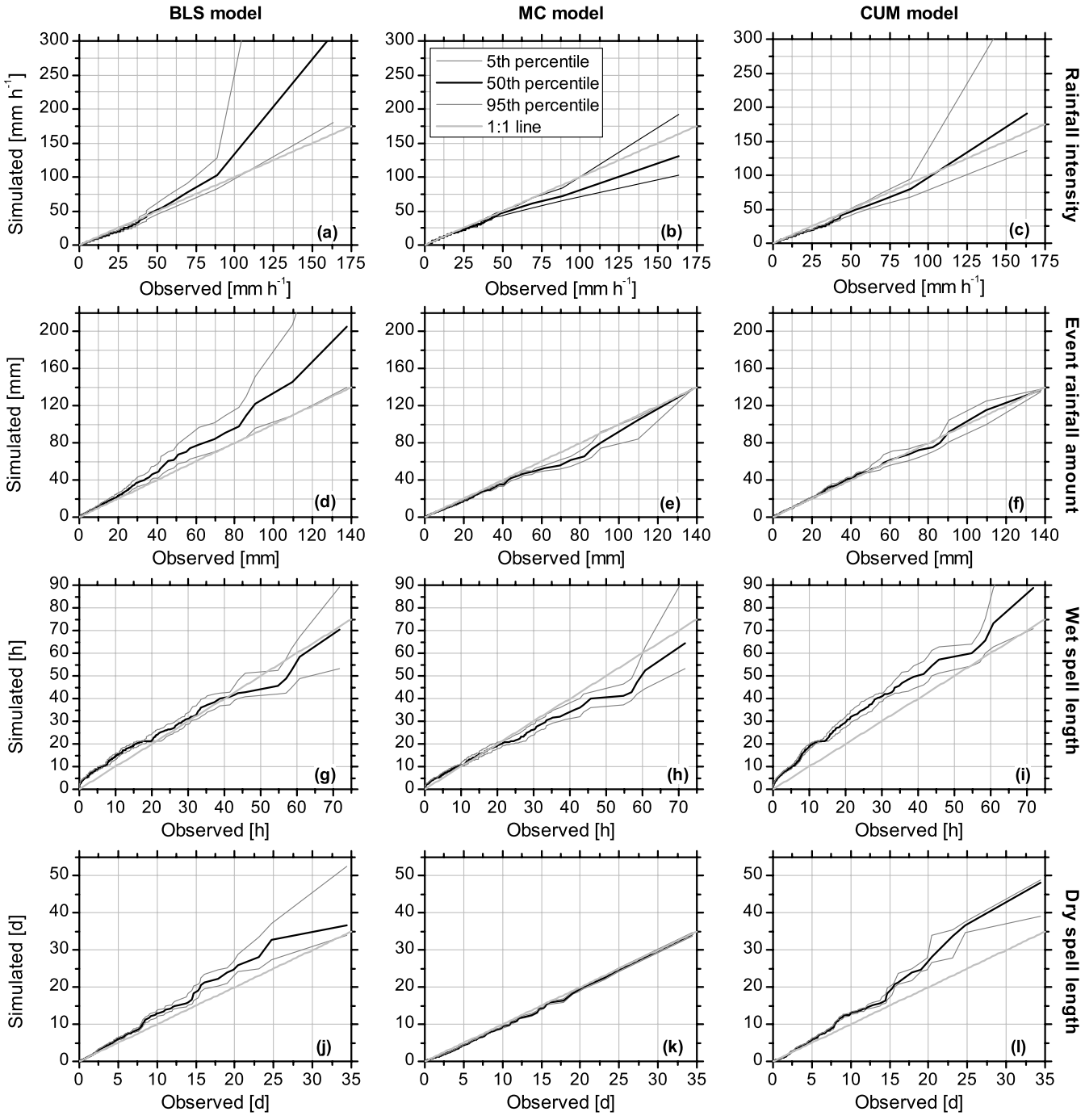

Fig. 7. QQ-plots of four physical summary statistics computed on 100 series simulated by BLS, MC, and CUM models. **(a)–(c)** Positive rainfall intensity at 5-min time scale. **(d)–(f)** Event rainfall amount. **(g)–(i)** Wet spell length. **(j)–(l)** Dry spell length. Grey lines denote the patterns of the median of each statistics computed on 100 simulations, while light grey lines are the 5th and 95th percentiles.

series that are able to mimic some physical properties of interest. Eight rainfall attributes were used for assessing the simulation quality: (1) positive rainfall ($R > 0$) at 5-min time scale; (2) rainfall accumulated during storm events; (3) wet spell durations; (4) dry spell durations; (5) percentage of zeros (no rain, P_0); (6) expectation of annual maxima; (7) standard deviation of annual maxima; (8) first 100 lags (≈8 h) of the autocorrelation function (ACF). To define independent storm events, a minimum critical inter-arrival time was computed by the method proposed by Restrepo-Posada and Eagleson (1982). The resulting values were 64, 23, and 29 h for CCE, MFI, and VIT, respectively. As these inter-arrival times

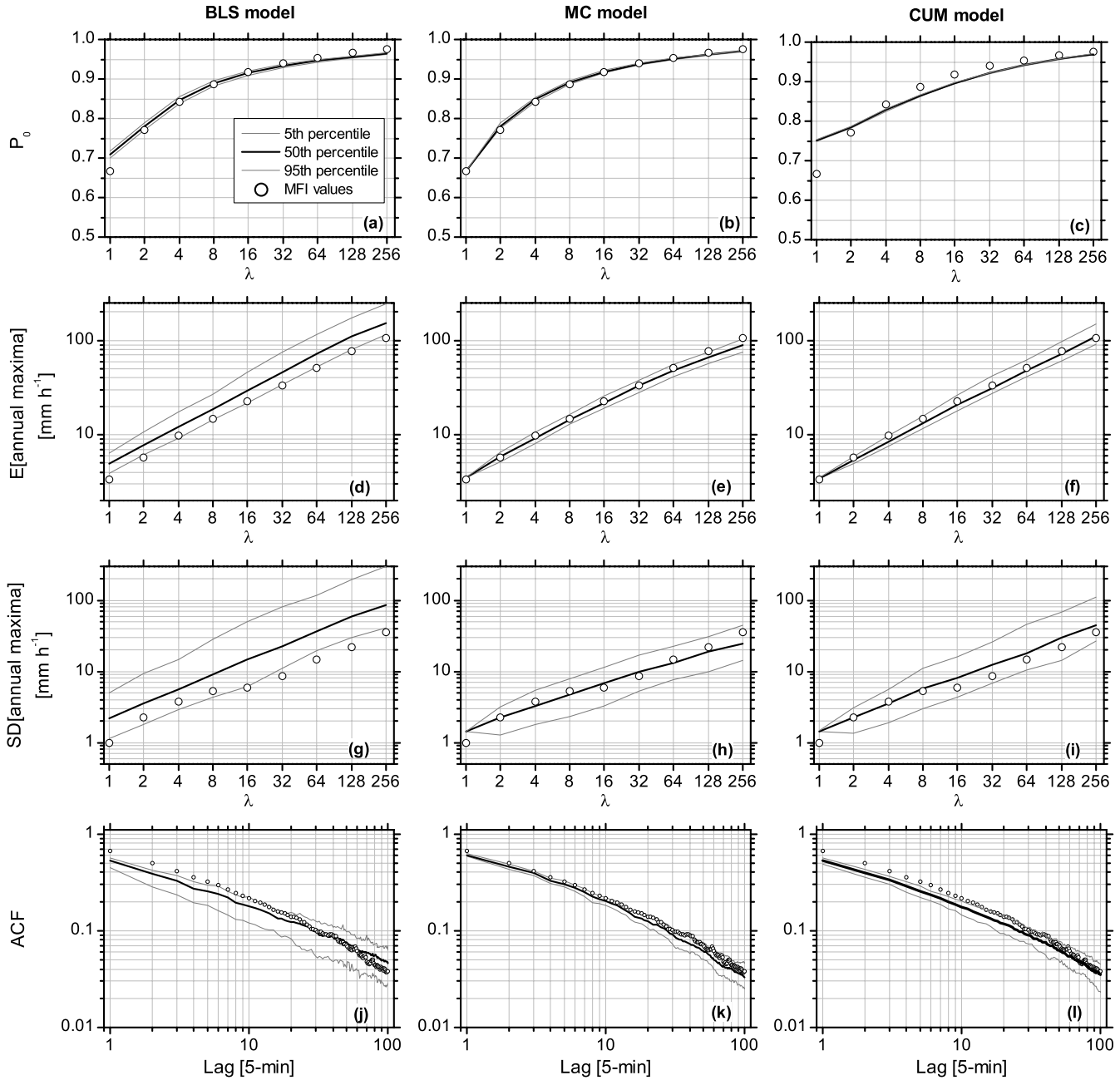

Fig. 8. Physical summary statistics computed on 100 series simulated by BLS, MC, and CUM models. **(a)–(c)** Probabilities of zero rainfall P_0. **(d)–(f)** Mean $E[\cdot]$ of annual maxima. **(g)–(i)** Standard deviation $SD[\cdot]$ of annual maxima. **(j)–(l)** Autocorrelation function. Grey lines denote the patterns of the median of each statistics computed on 100 simulations, while light grey lines are the 5th and 95th percentiles.

were longer than the typical evolution time of the storms for the specific climatic region (≈5–6 h on an average), a value of seven hours was adopted. This value is equal to or coherent with that applied by Salvadori and De Michele (2001) for a similar climate, and by Koutsoyiannis and Pachakis (1996) and Pathirana et al. (2003) for different climates.

The qq-plots in Fig. 7a–c show that the BLS model overestimates 5-min positive rainfall above $\approx 50\,\mathrm{mm\,h^{-1}}$, the MC model slightly underestimates the high quantiles, and the CUM model provides the most accurate median pattern. Moreover, high BLS and CUM quantiles are more dispersed than MC, reflecting the different models' structures. In fact, BLS and CUM models allow simulation of unbounded singularities, while MC model at the most preserves all mass contained in a time interval at coarse scales, resulting in bounded singularities. Focusing on the distributions of event

accumulated rainfall (Fig. 7d–f), BLS model overestimates this attribute and its variability, whereas MC and CUM models reproduce it rather accurately. Moreover, the uncertainty of the high MC and CUM quantiles is almost null and void. This behavior can be related to the distributions of positive values in Fig. 7a–c: extreme BLS and CUM quantiles show similar variability and different bias, while extreme MC and CUM quantiles show different variability (bounded and unbounded singularities) and similar (small) bias. As the event rainfall amount results from an integral process, the lack of bias plays a prominent role compared to presence/absence of isolated extreme realizations.

The BLS and CUM models tend to overestimate the wet spell length (Fig. 7g–i) for short durations (say, less than few hours), meaning that the simulated series tend to exhibit short events, which are longer than the corresponding observed events with equal probability. Since short durations refer to the events of main interest for studies concerning small basins, this property of the BLS and CUM series has to be taken into account in hydrological applications. On the other hand, the MC model reproduces wet spell durations less than $\approx$20 h rather well, but it slightly underestimates wet spells of longer durations (Fig. 7h). The BLS and CUM models tend to overestimate inter-arrival times, while the MC gives dry spells almost identical to the observed ones (Fig. 7j–l) owing to the exact mass preservation involved in the MC structure.

All models can simulate synthetic sequences with a percentage of zeros comparable to the observed one at 5-min scale (Fig. 8a–c). However, at the other coarser time scales, CUM model is outperformed by BLS and MC models that explicitly account for this property. The overestimation of P_0 by the BLS model at the coarsest reference time scale (Fig. 8i) is coherent with the results obtained by Molnar and Burlando (2005) for analogous canonical models based on lognormal distribution, while the MC model reproduces the exact P_0 owing to the exact preservation of the mass (Fig. 8j). The median patterns of the mean and standard deviation of the annual maxima across time scales (Fig. 8d–i) are reproduced more accurately by the MC and CUM models than by the BLS model, which also exhibits a higher variability than its competitors. Finally, the BLS model underestimates the ACF for the first 40 lags ($\approx$ 3 h, Fig. 8j), whereas the MC model provides more accurate ACF values (Fig. 8k). The ACF patterns of CUM and BLS are similar, the latter showing higher variability.

4.3 A look at nonlinear dynamics

In the last 25 years there has been an increasing interest in interpreting and modeling the rainfall series as chaotic nonlinear (possibly low-dimensional) dynamic systems rather than infinite-dimensional stochastic processes (e.g., Sivakumar et al., 2001, and references therein). As some rainfall series seem to support the presence of chaotic-deterministic behavior (e.g., Sivakumar et al., 1999; Dhanya and Nagesh Kumar, 2010), and some do not (e.g., Koutsoyiannis and Pachakis, 1996; Sivakumar et al., 2006), the analysis of continuous rainfall records has not yielded conclusive answers yet. The detection of chaotic behavior is usually performed by analyzing the correlation dimension D_2 computed via the Grassberger-Procaccia algorithm (e.g., Takens, 1981; Grassberger and Procaccia, 1983), based on the phase space reconstruction theorem (Takens, 1981). However, this approach is affected by a number of sources of error, such as the presence of lacunarity (see e.g., Theiler, 1990, for an overview). As the rainfall time series at fine time scales (say, ≤ 1 day) are characterized by a high percentage of zeros, the Grassberger-Procaccia algorithm may not be well-suited for these data (see e.g., Sivakumar, 2005; Koutsoyiannis, 2006, for a discussion on the effects of zeros on chaos detection in rainfall series).

Aiming at assessing the differences between observed and simulated series in terms of the possible chaotic behavior, we recall that the trajectories of the chaotic systems are virtually unpredictable because errors in measurement of the initial state propagate exponentially fast. As the Lyapunov exponents measure the rate of divergence, the largest Lyapunov exponent is a suitable index to identify a chaotic system. Referring the readers to Parker and Chua (1987) and Schreiber (1999) for practical introductions, here, it is mentioned that the largest Lyapunov exponent was estimated by the algorithm introduced by Rosenstein et al. (1993), based on the quantity:

$$\Xi(\Delta t) = \frac{1}{N}\sum_{t_0}^{N} \log\left(\frac{1}{\left|U(\xi_{t_0})\right|} \sum_{s_t \in U(\xi_{t_0})} \left|\xi_{t_0+\Delta t} - \xi_{t+\Delta t}\right| \right), \tag{20}$$

where ξ_{t_0} denotes the reference points, $U(\xi_{t_0})$ is the ball of radius ϵ centered at the point ξ_{t_0}. The presence of possible chaotic dynamics results in an increasing linear pattern of $\Xi(\Delta t)$ for a reasonable range of ϵ and for all the embedding dimensions m larger than some minimum dimension m_0, and the positive slope of this linear pattern is an estimate of the largest Lyapunov exponent. We have used $\epsilon = 480$ 5-min intervals = 40 h, which is equal to the decorrelation time (i.e., the first lag at which ACF becomes zero) and $m = \{10, 25\}$. The patterns of $\Xi(\Delta t)$ in Fig. 9 show that any scaling linear region is present either in the observed or representative simulated series. This denotes that there is no evidence for the divergence of trajectories in the reconstructed phase space, and thus for chaotic behavior. Of course, the use of a unique index to detect chaos is not enough (e.g., Dhanya and Nagesh Kumar, 2010); however, the essential point is that the BLS, MC, and CUM series, all reproduce MFI patterns rather well, but for some intrinsic statistical fluctuations. Hence, for the data on hand, stochastic models represent a reasonable way to describe and simulate 5-min rainfall series.

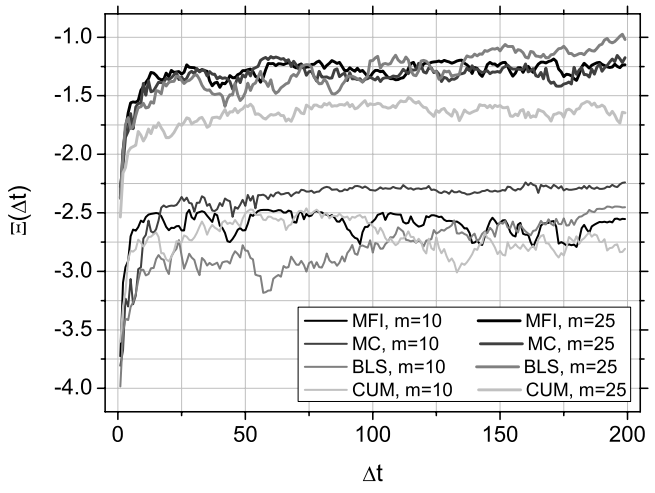

Fig. 9. $\Xi(\Delta t)$ patterns for the embedding dimensions m equal to 10 and 25 (see text for details).

5 Conclusions

The analysis of rainfall series at 5-min resolution has pointed out that the weights W characterizing the discrete random cascade models used to describe the rainfall process do not appear to be iid. The generator W exhibits a complex dependence on scale and rainfall intensity (or amount), which is reflected in the behavior of the parameters of the discrete models considered in this study (MC and BLS). In order to explore the nature of these departures from the iid hypothesis, we have introduced the above-mentioned dependences in the models' parameterization by a set of suitable, simple functions. Moreover, the physically based CUM model was used as a benchmark model to check the consistency of the departures from multifractality. The models were tested by comparing a number of statistics computed on the observed and simulated series. The results can be summarized as follows:

1. The series simulated by discrete BLS and MC models can reproduce the analytical relationships that characterize the models, and synthesize departures of W from the iid hypothesis. The BLS model tends to give biased estimates more than the MC model does. This could be ascribed to the differences between the bare and dressed processes (e.g., Veneziano et al., 2006; Paulson and Baxter, 2007), which were not corrected during the model calibration. However, if this is the case, MC model appears to be less sensible than BLS model to bare/dressed bias.

2. The patterns that describe the dependence of BLS and MC parameters on scale level and rainfall intensity (or amount) can be also reproduced by CUM model, which was properly thresholded to account for zero rainfall measurements. Therefore, the detection of these patterns is not sufficient to establish whether the departure from multifractality is real or it has to be ascribed to measurement inaccuracy. Moreover, we cannot exclude that the scale by scale changes in the parameters may depend on the use of cascade weights estimated by conditioning to the rainfall intensity (amount) at the parent time intervals (Eq. 6). This approach implicitly involves a microcanonical conservation which may cause, to some extent, the systematic patterns of the models' parameters.

3. The multifractal analysis of the observed and simulated series confirms that BLS model tends to yield biased results, whereas MC and CUM models yield rather accurate results. In particular, it is shown that the simple thresholding procedure applied to CUM series is able to reproduce the shape of the observed scaling exponent function.

4. Results concerning the physical summary statistics confirm the satisfactory performance of MC and CUM models. Since the latter model implies unbounded singularities, it provides larger extreme realizations than the MC model. Nevertheless, the MC model allows for a more accurate simulation of some properties, such as wet/dry spells, ACF, and probability of zero rainfall at the scales of interest. Even though the MC model discussed in this study is not physically based and not multifractal at all, the properties of the simulated series can explain the interest for its study and possible application to real-world problems.

5. The patterns of the largest Lyapunov exponent point out that there are no substantial differences between the observed and simulated series, and there is no evidence for low-dimensional nonlinear dynamics driving the analyzed rainfall series.

Finally, it is worth bearing in mind that the results presented in this study depend on the analyzed data as pointed out by the variety of conclusions available in the literature focusing on these topics. However, a twofold overall conclusion can be drawn: (1) the departures from multifractal behavior on real-world rainfall data can be explained in different ways, making difficult definitive statements. Of course, in agreement to the Occam's razor, the simplest and theoretically/physically based explanation should be preferred. (2) From the practical point of view, the choice of a model is related to the scope of the analysis; even though the theoretically/physically based models should be preferred, other options should not be discarded a priori, as they can provide suitable solutions for specific problems.

Acknowledgements. The author thanks the Editor Shaun Lovejoy (McGill University, Canada), Roberto Deidda (Università di Cagliari, Italy), and an anonymous reviewer for their constructive criticisms and insightful comments that helped to greatly improve

the quality of the original manuscript. The work was carried out partly under the project "Preliminary study of hydraulic risk within the basins of Rio Torbido, Torrente Rigo, Torrente Vezza, and related sub-basins located in Viterbo administrative province" supported by Provincia di Viterbo and Tiber River Basin Authority.

Edited by: S. Lovejoy
Reviewed by: R. Deidda and another anonymous referee

References

Deidda, R.: Rainfall downscaling in a space-time multifractal framework, Water Resour. Res., 36, 1779–1794, doi:10.1029/2000WR900038, 2000.

Deidda, R., Benzi, R., and Siccardi, F.: Multifractal modeling of anomalous scaling laws in rainfall, Water Resour. Res., 35, 1853–1867, doi:10.1029/1999WR900036, 1999.

Deidda, R., Badas, M. G., and Piga, E.: Space-time multifractality of remotely sensed rainfall fields, J. Hydrol., 322, 2–13, doi:10.1016/j.jhydrol.2005.02.036, 2006.

de Lima, M. I. P. and de Lima, J. L. M. P.: Investigating the multifractality of point precipitation in the Madeira archipelago, Nonlin. Processes Geophys., 16, 299–311, doi:10.5194/npg-16-299-2009, 2009.

de Lima, M. I. P. and Grasman, J.: Multifractal analysis of 15-min and daily rainfall from a semi-arid region in Portugal, J. Hydrol., 220, 1–11, doi:10.1016/S0022-1694(99)00053-0, 1999.

Dennis Jr., J. E., Gay, D. M., and Welsch, R. E.: Algorithm 573: NL2SOL–An adaptive nonlinear least-squares algorithm [E4], ACM Transactions on Mathematical Software, 7, 369–383, 1981.

Dhanya, C. T. and Nagesh Kumar, D.: Nonlinear ensemble prediction of chaotic daily rainfall, Adv. Water Resour., 33, 327–347, 2010.

Gaume, E., Mouhous, N., and Andrieu, H.: Rainfall stochastic disaggregation models: Calibration and validation of a multiplicative cascade model, Adv. Water Resour., 30, 1301–1319, 2007.

Grassberger, P. and Procaccia, I.: Characterization of strange attractors, Phys. Rev. Lett., 50, 346–349, 1983.

Güntner, A., Olsson, J., Calver, A., and Gannon, B.: Cascade-based disaggregation of continuous rainfall time series: the influence of climate, Hydrol. Earth Syst. Sci., 5, 145–164, doi:10.5194/hess-5-145-2001, 2001.

Gupta, V. and Waymire, E.: A statistical analysis of mesoscale rainfall as a random cascade, J. Appl. Meteorol., 32, 251–267, 1993.

Harris, D., Seed, A., Menabde, M., and Austin, G.: Factors affecting multiscaling analysis of rainfall time series, Nonlin. Processes Geophys., 4, 137–155, doi:10.5194/npg-4-137-1997, 1997.

Kolmogorov, A. N.: The local structure of turbulence in incompressible viscous fluid for very large Reynolds numbers, Proceedings of the USSR Academy of Sciences, 30, 299–303, 1941.

Kolmogorov, A. N.: The local structure of turbulence in incompressible viscous fluid for very large Reynolds numbers, Proceeding of Royal Society of London, Series A, 434, 9–13, 1991.

Koutsoyiannis, D.: On the quest for chaotic attractors in hydrological processes, Hydrolog. Sci. J., 51, 1065–1091, 2006.

Koutsoyiannis, D. and Pachakis, D.: Deterministic chaos versus stochasticity in analysis and modeling of point rainfall series, J. Geophys. Res., 101, 26441–26451, doi:10.1029/96JD01389, 1996.

Koutsoyiannis, D. and Xanthopoulos, T.: A dynamic model for short-scale rainfall disaggregation, Hydrolog. Sci. J., 35, 303–322, 1990.

Koutsoyiannis, D., Onof, C., and Wheater, H. S.: Multivariate rainfall disaggregation at a fine time scale, Water Resour. Res., 39, 1173, doi:10.1029/2002WR001600, 2003.

Lavallée, D., Schertzer, D., and Lovejoy, S.: On the determination of the codimension function, in: Scaling, fractals and non-linear variability in geophysics, edited by: Schertzer, D. and Lovejoy, S., pp. 99–110, Kluwer, 1991.

Lovejoy, S. and Schertzer, D.: Multifractals and Rain, in: New Uncertainty Concepts in Hydrology and Hydrological modelling, edited by: Kundzewicz, A. W., pp. 62–103, Cambridge University Press, Cambridge, 1995.

Lovejoy, S. and Schertzer, D.: On the simulation of continuous in scale universal multifractals, part I: spatially continuous processes, Computers and Geoscience, 36, 1393–1403, doi:10.1016/j.cageo.2010.04.010, 2010a.

Lovejoy, S. and Schertzer, D.: On the simulation of continuous in scale universal multifractals, part II: space-time processes and finite size corrections, Computers and Geoscience, 36, 1404–1413, doi:10.1016/j.cageo.2010.07.001, 2010b.

Lovejoy, S., Schertzer, D., and Allaire, V. C.: The remarkable wide range spatial scaling of TRMM precipitation, Atmos. Res., 90, 10–32, doi:10.1016/j.atmosres.2008.02.016, 2008.

Mandelbrot, B. B.: Intermittent turbulence in self-similar cascades: divergence of high moments and dimension of the carrier, J. Fluid Mech., 62, 331–358, 1974.

Mascaro, G., Vivoni, E. R., and Deidda, R.: Downscaling soil moisture in the southern Great Plains through a calibrated multifractal model for land surface modeling applications, Water Resour. Res., 46, W08546, doi:10.1029/2009WR008855, 2010.

Menabde, M. and Sivapalan, M.: Modeling of rainfall time series and extremes using bounded random cascades and Levy-stable distributions, Water Resour. Res., 36, 3293–3300, 2000.

Menabde, M., Harris, D., Seed, A., Austin, G., and Stow, D.: Multiscaling properties of rainfall and bounded random cascades, Water Resour. Res., 33, 2823–2830, 1997.

Molnar, P. and Burlando, P.: Preservation of rainfall properties in stochastic disaggregation by a simple random cascade model, Atmos. Res., 77, 137–151, 2005.

Mood, A. M., Graybill, F. A., and Boes, D. C.: Introduction to the Theory of Statistics, McGraw-Hill, New York, 3rd edn., 1974.

Olsson, J.: Limits and characteristics of the multifractal behavior of a high-resolution rainfall time series, Nonlin. Processes Geophys., 2, 23–29, doi:10.5194/npg-2-23-1995, 1995.

Olsson, J.: Evaluation of a scaling cascade model for temporal rain-fall disaggregation, Hydrol. Earth Syst. Sci., 2, 19–30, doi:10.5194/hess-2-19-1998, 1998.

Olsson, J. and Berndtsson, R.: Temporal rainfall disaggregation based on scaling properties, Water Sci. Technol., 37, 73–79, 1998.

Onof, C., Townend, J., and Kee, R.: Comparison of two hourly to 5-min rainfall disaggregators, Atmos. Res., 77, 176–187, 2005.

Over, T. M. and Gupta, V. K.: Statistical analysis of masoscale rainfall: Dependence of a random cascade generator on large-scale forcing, J. Appl. Meteorol., 33, 1526–1542, 1994.

Over, T. M. and Gupta, V. K.: A space-time theory of mesoscale rainfall using random cascades, J. Geophys. Res., 101, 26319–26331, 1996.

Parker, T. and Chua, L.: Chaos: A tutorial for engineers, Proceedings of the IEEE, 75, 982–1008, 1987.

Pathirana, A., Herath, S., and Yamada, T.: Estimating rainfall distributions at high temporal resolutions using a multifractal model, Hydrol. Earth Syst. Sci., 7, 668–679, doi:10.5194/hess-7-668-2003, 2003.

Paulson, K. S. and Baxter, P. D.: Downscaling of rain gauge time series by multiplicative beta cascade, J. Geophys. Res., 112, D09105, doi:10.1029/2006JD007333, 2007.

R Development Core Team: R: A Language and Environment for Statistical Computing, R Foundation for Statistical Computing, Vienna, Austria, http://www.R-project.org, ISBN 3-900051-07-0, 2009.

Restrepo-Posada, P. J. and Eagleson, P. S.: Identification of independent rainstorms, J. Hydrol., 55, 303–319, 1982.

Rosenstein, M. T., Collins, J. J., and De Luca, C. J.: A practical method for calculating largest Lyapunov exponents from small data sets, Physica D, 65, 117–134, 1993.

Royer, J.-F., Biaou, A., Chauvin, F., Schertzer, D., and Lovejoy, S.: Multifractal analysis of the evolution of simulated precipitation over France in a climate scenario, Comptes Rendus Geosciences, 340, 431–440, doi:10.1016/j.crte.2008.05.002, 2008.

Rupp, D. E., Keim, R. F., Ossiander, M., Brugnach, M., and Selker, J. S.: Time scale and intensity dependency in multiplicative cascades for temporal rainfall disaggregation, Water Resour. Res., 45, W07409, doi:10.1029/2008WR007321, 2009.

Salvadori, G. and De Michele, C.: From Generalized Pareto to Extreme Values laws: Scaling properties and derived features, J. Geophys. Res., 106, 24063–24070, 2001.

Samorodnitsky, G. and Taqqu, M. S.: Stable Non-Gaussian Random Processes, Chapman & Hall, New York, 1994.

Schertzer, D. and Lovejoy, S.: Physical modeling and analysis of rain and clouds by anisotropic scaling of multiplicative processes, J. Geophys. Res., 92, 9693–9714, 1987.

Schertzer, D. and Lovejoy, S.: Hard and Soft Multifractal processes, Physica A, 185, 187–194, 1992.

Schertzer, D. and Lovejoy, S.: Universal Multifractals do Exist!: Comments on "A statistical analysis of mesoscale rainfall as a random cascade", J. Appl. Meteorol., 36, 1296–1303, 1997.

Schertzer, D., Lovejoy, S., Lavallée, D., and Schmitt, F.: Universal hard multifractal turbulence, theory and observations, in: Nonlinear Dynamics of Structures, edited by: Sagdeev, R. Z., Frisch, U., Hussain, F., Moiseev, S. S., and Erokhin, N. S., pp. 213–235, World Scientific, 1991.

Schertzer, D., Tchiguirinskaia, I., Lovejoy, S., and Hubert, P.: No monsters, no miracles: in nonlinear sciences hydrology is not an outlier!, Hydrolog. Sci. J., 55, 965–979, 2010.

Schmitt, F., Lavallée, D., Schertzer, D., and Lovejoy, S.: Empirical determination of universal multifractal exponents in turbulent velocity fields, Phys. Rev. Lett., 68, 305–308, 1992.

Schmitt, F., Schertzer, D., Lovejoy, S., and Brunet, Y.: Estimation of universal multifractal indices for atmospheric turbulent velocity fields, Fractals, 1, 568–575, 1993.

Schreiber, T.: Interdisciplinary application of nonlinear time series methods, Physics Reports, 308, 1–64, 1999.

Serinaldi, F.: A multisite daily rainfall generator driven by bivariate copula-based mixed distributions, J. Geophys. Res., 114, D10103, doi:10.1029/2008JD011258, 2009.

Sivakumar, B.: Chaos in rainfall: variability, temporal scale and zeros, J. Hydroinform., 7, 175–184, 2005.

Sivakumar, B. and Sharma, A.: A cascade approach to continuous rainfall data generation at point locations, Stoch. Env. Res. Risk A., 22, 451–459, 2008.

Sivakumar, B., Liong, S. Y., Liaw, C. Y., and Phoon, K. K.: Singapore rainfall behavior: Chaotic?, J. Hydrol. Eng., 4, 38–48, 1999.

Sivakumar, B., Sorooshian, S., Gupta, H. V., and Gao, X.: A chaotic approach to rainfall disaggregation, Water Resour. Res., 37, 61–72, 2001.

Sivakumar, B., Wallender, W. W., Horwath, W. R., Mitchell, J. P., Prentice, S. E., and Joyce, B. A.: Nonlinear analysis of rainfall dynamics in California's Sacramento Valley, Hydrol. Processes, 20, 1723–1736, doi:10.1002/hyp.5952, 2006.

Takens, F.: Detecting strange attractors in turbulence, Lecture Notes in Mathematics, 898, 366–381, 1981.

Tessier, Y., Lovejoy, S., and Schertzer, D.: Universal multifractals: Theory and observations for rain and clouds, J. Appl. Meteorol., 32, 223–250, 1993.

Theiler, J.: Estimating fractal dimension, J. Opt. Soc. Am. A, 7, 1055–1073, 1990.

Veneziano, D. and Iacobellis, V.: Multiscaling pulse representation of temporal rainfall, Water Resour. Res., 38, 1138, doi:10.1029/2001WR000522, 2002.

Veneziano, D., Bras, R. L., and Niemann, J. D.: Nonlinearity and self-similarity of rainfall in time and a stochastic model, J. Geophys. Res., 101, 26371–26392, 1996.

Veneziano, D., Furcolo, P., and Iacobellis, V.: Imperfect scaling of time and space-time rainfall, J. Hydrol., 322, 105–119, 2006.

Wilson, J., Lovejoy, S., and Schertzer, D.: Physically based cloud modelling by scaling multiplicative cascade processes, in: Scaling, fractals and non-linear variability in geophysics, edited by: Schertzer, D. and Lovejoy, S., pp. 185–208, Kluwer, 1991.